INVESTIGATION OF FREE VIBRATION OF FGP PLATES PARTIALLY SUPPORTED BY ELASTIC FOUNDATION USING FINITE ELEMENT METHOD

PHÂN TÍCH DAO ĐỘNG RIÊNG CỦA TẤM FGM CÓ LỖ RỖNG (FGP) ĐẶT MỘT PHẦN TRÊN NỀN ĐÀN HỒI BẰNG PHƯƠNG PHÁP PHẦN TỬ HỮU HẠN

Nguyen Thi Dung[1,*]

DOI: https://doi.org/10.57001/huih5804.68

ABSTRACT

The main goal of this article is to use a finite element method (FEM) based on Mindlin plate theory for analyzing the free vibration of the functionally graded porous (FGP) plate partially supported by elastic foundation (EF). The EF is Pasternak foundation model includes spring stiffness (k_1) and shear layer stiffness (k_2). The FGP materials with two-parameter are the power-law index (k) and the porosity volume fraction (ξ) in two cases of even and uneven porosity. Some numerical results in our work are compared with other published to verify accuracy and reliability. Moreover, the effect of the elastic foundation on the free vibration of FGP plates is also fully investigated.

Keywords: *FEM, Functionally Graded Porous, Elastic Foundation, Rectangular plates.*

TÓM TẮT

Bài báo sử dụng phương pháp phần tử hữu hạn (FEM) dựa trên lý thuyết tấm Midlin để phân tích dao động tự do của tấm bằng vật liệu cơ tính biến thiên có lỗ rỗng (FGP) được đặt một phần trên nền đàn hồi (EF). Nền đàn hồi là nền Pasternak gồm có độ cứng lò xo k_1 và độ cứng lớp chống cắt k_2. Vật liệu xốp FGP gồm hai tham số là chỉ số mũ thể tích (k) và hệ số phân bố lỗ rỗng (ξ). Các kết quả tính toán lý thuyết cũng như chương trình tính toán số đã được tác giả so sánh với một số kết quả của các tác giả khác đã được công bố để xác minh độ tin cậy và chính xác. Bên cạnh đó, các tính toán số được thực hiện nhằm đánh giá ảnh hưởng của nền đàn hồi tới dao động tự do của tấm FGP cũng được nghiên cứu và trình bày đầy đủ.

Từ khóa: *Phương pháp phần tử hữu hạn FEM, tấm xốp cơ tính biến thiên, tấm chữ nhật.*

[1]Faculty of Mechanical Engineering, Le Quy Don Technical University
[*]Email: dung28688@gmail.com
Received: 20/8/2022
Revised: 15/10/2022
Accepted: 22/11/2022

1. INTRODUCTION

The plate structures resting on the EF are common in practice and attract many scientists around the world to focus on research. Some typical works can be summarized as Li *et al.* [1] examined the nonlinear vibration of FGP sandwich plates using Galerkin and the fourth-order Runge-Kutta methods. Zenkour *et al.* [2] proposed a four-unknown variable plate theory for the vibration analysis of composite/sandwich plates. Duc and his colleagues investigated the nonlinear dynamic problem of FGM plates [3] and FGM shells lying on the EF [4]. Moreover, the numerical results of the mechanical response of FGM structures are shown in his book [5]. Mahmoudi and coworkers [6] used a refined Quasi-3D theory to study the bending of FG sandwich plates resting on Winkler-Pasternak foundation. Omurtag and coworkers [7] employed mixed finite element formulation based on gateaux differential to investigate the free vibration of thin plates. Zhou and coworkers [8] employed the Ritz method to study the dynamic response of rectangular thick plates while Ferreira *et al*. [9] used radial basis functions for bending and vibration analysis of rectangular plates. In addition, valuable numerical results about mechanical analysis of structures lying on the elastic foundation can be found in [10-12]. Motaghian and partners [13] computed the free vibration of plates partially supported EF using the analytical solution.

In this research, authors extend the eight-node quadrilateral (Q8) element combined with Mindlin plate theory to more accurately describe the stress-strain and displacement field of the FGP plate. The accuracy and reliability of the present approach are verified by comparing numerical results with other previous publications. Moreover, the effects of foundation parameters and material properties on the free vibration of FGP plates are examined in detail.

2. GOVENING EQUANTIONS

2.1. The FGP plate

In this research, we consider a rectangular FGP plate with the length a, the width b and the thickness h partially supported by EF as shown in Fig. 1. The EF consists of two types is Type 1: The EF with the rectangular domain follows

vertical as Fig. 2(a); and Type 2: The PSEF with the rectangular domain follows horizontal as Fig. 2(b). Note that the area of EF in these types is the same.

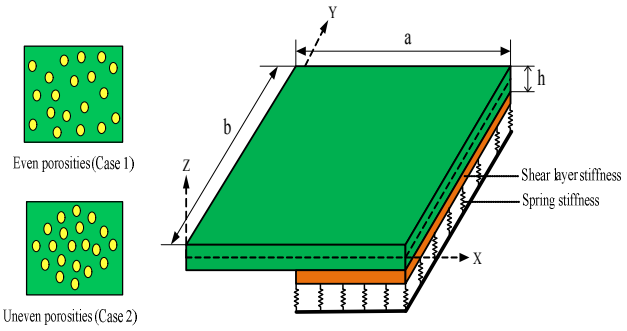

Fig. 1. Model of FGP plates partially supported by EF.

(a) The FGP plate, (b) Even porosity, (c) Uneven porosity

The FGP materials with a variation of two constituents and two different distributions of porosity through-thickness are determined by [14]:

$$\text{Case 1: } P(z) = P_m + (P_c - P_m)\left(\frac{z}{h} + 0,5\right)^k - \frac{\xi}{2}(P_c + P_m) \quad (1)$$

Case 2:

$$P(z) = P_m + (P_c - P_m)\left(\frac{z}{h} + 0,5\right)^k - \frac{\xi}{2}(P_c + P_m)\left(1 - \frac{2|z|}{h}\right) \quad (2)$$

Where P represents any effective material property such as Young's modulus E, mass density ρ, and Poisson's ratio υ; k is the volume fraction index, ξ ($\xi \le 1$) represents the porosity volume fraction. Subscripts m and c denote the metallic and ceramic constituents, respectively.

The force acting of The Winkler-Pasternak foundation is given by [14]:

$$q_e = k_1 w - k_2\left(\frac{\partial^2 w}{\partial x^2} + \frac{\partial^2 w}{\partial y^2}\right) \quad (3)$$

With w is the displacement of the plate along the z-axis; k_1, k_2 are spring stiffness and shear layer stiffness, respectively.

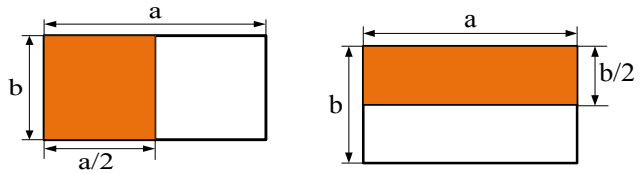

(a) Type 1 (b) Type 2

Fig. 2. Different types of EF

2.2. The displacement field

According to the first-order shear deformation theory (FSDT), the displacement field of the FGP plate is given by [15]:

$$u(x,y,z) = u_0(x,y) + z\theta_y(x,y);$$
$$v(x,y,z) = v_0(x,y) + z\theta_x(x,y);\ w(x,y,z) = w_0(x,y) \quad (4)$$

with u_0, v_0, w_0 are the displacement components at the mid-plane (z = 0) along x, y, z-axis; θ_x, θ_y are the angle of rotation of the mid-surface about the y and x-axis, respectively.

2.3. The strain vector

The strain vector of the plate is defined according to the displacement field as follows:

$$\boldsymbol{\varepsilon} = \begin{Bmatrix} \varepsilon_{xx} \\ \varepsilon_{yy} \\ \varepsilon_{xy} \\ \varepsilon_{xz} \\ \varepsilon_{yz} \end{Bmatrix} = \begin{Bmatrix} u_{,x} \\ v_{,y} \\ u_{,y} + v_{,x} \\ w_{,x} + u_{,z} \\ w_{,y} + v_{,z} \end{Bmatrix} = \begin{Bmatrix} u_{0,x} \\ v_{0,y} \\ u_{0,y} + v_{0,x} \\ v_{0,x} + \theta_x \\ w_{0,y} + \theta_y \end{Bmatrix} + z\begin{Bmatrix} \theta_{x,x} \\ \theta_{y,y} \\ \theta_{x,y} + \theta_{y,x} \\ 0 \\ 0 \end{Bmatrix} \quad (5)$$

$$\boldsymbol{\varepsilon} = \{\boldsymbol{\varepsilon}_1 \quad \boldsymbol{\varepsilon}_2\}^T = \{\boldsymbol{\varepsilon}_1^0 + z\boldsymbol{\varepsilon}_1^1 \quad \boldsymbol{\varepsilon}_2^0\}^T \quad (6)$$

with

$$\boldsymbol{\varepsilon}_1 = \begin{Bmatrix} \varepsilon_{xx} \\ \varepsilon_{yy} \\ \varepsilon_{xy} \end{Bmatrix}; \boldsymbol{\varepsilon}_2 = \begin{Bmatrix} \varepsilon_{xz} \\ \varepsilon_{yz} \end{Bmatrix}; \boldsymbol{\varepsilon}_1^0 = \begin{Bmatrix} u_{0,x} \\ v_{0,y} \\ u_{0,y} + v_{0,x} \end{Bmatrix};$$
$$\boldsymbol{\varepsilon}_1^1 = \begin{Bmatrix} \theta_{x,x} \\ \theta_{y,y} \\ \theta_{x,y} + \theta_{y,x} \end{Bmatrix}; \boldsymbol{\varepsilon}_2^0 = \begin{Bmatrix} w_{0,x} + \theta_x \\ w_{0,y} + \theta_y \end{Bmatrix} \quad (7)$$

2.4. The stress-strain relation

The tress-strain relation is defined by

$$\boldsymbol{\sigma} = \mathbf{D}.\boldsymbol{\varepsilon} \quad (8a)$$

$$\mathbf{D} = \begin{bmatrix} \mathbf{D}_b & \mathbf{0}_{3\times 2} \\ \mathbf{0}_{2\times 3} & \mathbf{D}_s \end{bmatrix}; \mathbf{D}_b = \begin{bmatrix} C_{11} & C_{12} & 0 \\ & C_{22} & 0 \\ \text{sym} & & C_{66} \end{bmatrix}; \quad (8b)$$

$$\mathbf{D}_s = \begin{bmatrix} C_{55} & 0 \\ 0 & C_{44} \end{bmatrix}$$

$$C_{11} = C_{22} = \frac{E}{(1-\upsilon^2)}; C_{12} = \frac{\upsilon E}{(1-\upsilon^2)};$$
$$C_{66} = C_{55} = C_{44} = \frac{E}{2(1+\upsilon)} \quad (9)$$

The relationship between the internal forces and the deformation components are written in the form:

$$\{N_{xx} \quad N_{yy} \quad N_{xy}\} = \mathbf{A}\boldsymbol{\varepsilon}_1^0 + \mathbf{B}\boldsymbol{\varepsilon}_1^1;$$
$$\{M_{xx} \quad M_{yy} \quad M_{xy}\} = \mathbf{B}\boldsymbol{\varepsilon}_1^0 + \mathbf{X}\boldsymbol{\varepsilon}_1^1; \{Q_{xz} \quad Q_{yz}\} = \mathbf{A}^s\boldsymbol{\varepsilon}_2^0 \quad (10)$$

where $\mathbf{A}$; $\mathbf{B}$; $\mathbf{X}$; $\mathbf{A}^s$ are defined as follows

$$(\mathbf{A}; \mathbf{B}; \mathbf{X}) = \int_{-h/2}^{h/2} \mathbf{D}_b.(1; z; z^2)\,dz; \ \mathbf{A}^s = \frac{5}{6}\int_{-h/2}^{h/2} \mathbf{D}_s.dz \quad (11)$$

2.5. The plate element

The eight-node plate element type is used. Each node has five degrees of freedom (DOF). The 4.0-dimentional nodal displacement vector is:

$$\mathbf{d}_e = [\mathbf{d}_1^T \quad \mathbf{d}_2^T \quad \mathbf{d}_3^T \quad \mathbf{d}_4^T \quad \mathbf{d}_5^T \quad \mathbf{d}_6^T \quad \mathbf{d}_7^T \quad \mathbf{d}_8^T]^T \tag{12}$$

The displacements at the node i (i = 1 ÷ 8) of element is expressed byl

$$\mathbf{d}_i = \{u_{0i} \quad v_{0i} \quad w_{0i} \quad \varphi_{xi} \quad \varphi_{yi}\} \tag{13}$$

The displacement field in each plate element is interpolated through the node displacement as follows

$$\begin{aligned} &u_0 = \mathbf{N}_u.\mathbf{d}_e;\ v_0 = \mathbf{N}_v.\mathbf{d}_e;\ w_0 = \mathbf{N}_w.\mathbf{d}_e; \\ &\varphi_x = \mathbf{N}_{\varphi x}.\mathbf{d}_e;\ \varphi_y = \mathbf{N}_{\varphi y}.\mathbf{d}_e \end{aligned} \tag{14}$$

here $\mathbf{N}_u, \mathbf{N}_v, \mathbf{N}_w, \mathbf{N}_{\varphi x}, \mathbf{N}_{\varphi y}$ are the shape functions [16].

$$\begin{cases} \mathbf{N}_u = \left[\mathbf{N}_1^{(1)} \quad \mathbf{N}_2^{(1)} \quad \ldots \quad \mathbf{N}_7^{(1)} \quad \mathbf{N}_8^{(1)}\right]; \\ \mathbf{N}_v = \left[\mathbf{N}_1^{(2)} \quad \mathbf{N}_2^{(2)} \quad \ldots \quad \mathbf{N}_7^{(2)} \quad \mathbf{N}_8^{(2)}\right]; \\ \mathbf{N}_w = \left[\mathbf{N}_1^{(3)} \quad \mathbf{N}_2^{(3)} \quad \ldots \quad \mathbf{N}_7^{(3)} \quad \mathbf{N}_8^{(3)}\right]; \\ \mathbf{N}_{\varphi x} = \left[\mathbf{N}_1^{(4)} \quad \mathbf{N}_2^{(4)} \quad \ldots \quad \mathbf{N}_7^{(4)} \quad \mathbf{N}_8^{(4)}\right]; \\ \mathbf{N}_{\varphi y} = \left[\mathbf{N}_1^{(5)} \quad \mathbf{N}_2^{(5)} \quad \ldots \quad \mathbf{N}_7^{(5)} \quad \mathbf{N}_8^{(5)}\right]. \end{cases} \tag{15}$$

The matrices $\mathrm{N}_i^{(j)}\ (j = 1 \div 5)$ are given by

$$\begin{cases} \mathbf{N}_i^{(1)} = [\psi_i \quad 0 \quad 0 \quad 0 \quad 0]; \mathbf{N}_i^{(2)} = [0 \quad \psi_i \quad 0 \quad 0 \quad 0]; \\ \mathbf{N}_i^{(3)} = [0 \quad 0 \quad \psi_i \quad 0 \quad 0]; \mathbf{N}_i^{(4)} = [0 \quad 0 \quad 0 \quad \psi_i \quad 0]; \\ \mathbf{N}_i^{(5)} = [0 \quad 0 \quad 0 \quad 0 \quad \psi_i]. \end{cases} \tag{16}$$

where ψ_i is the Lagrange interpolation function.

The element stiffness matrix is determined by

$$\mathbf{K}_e = \mathbf{K}_e^b + \mathbf{K}_e^s + \mathbf{K}_e^f \tag{17}$$

with $\mathbf{K}_e^b, \mathbf{K}_e^s$ are the bending, shear element stiffness matrices, respectively.

Those matrices are determined as follows:

$$\mathbf{K}_e^b = \int_{S_e} \left(\begin{bmatrix} \mathbf{B}_1^T & \mathbf{B}_2^T \end{bmatrix} \begin{bmatrix} \mathbf{A} & \mathbf{B} \\ \mathbf{B} & \mathbf{X} \end{bmatrix} \begin{bmatrix} \mathbf{B}_1 \\ \mathbf{B}_2 \end{bmatrix} \right) dxdy \tag{18}$$

$$\mathbf{K}_e^s = \frac{5}{6} \int_{S_e} \left(\mathbf{B}_3^T \mathbf{A}^s \mathbf{B}_3 \right) dxdy \tag{19}$$

$$\mathbf{K}_e^f = \int_{S_e} (k_1 \mathbf{N}_w^T \mathbf{N}_w + k_2 (\mathbf{N}_{w,x}^T \mathbf{N}_{w,x} + \mathbf{N}_{w,y}^T \mathbf{N}_{w,y})) dxdy \tag{20}$$

where

$$\mathbf{B}_1 = \begin{bmatrix} \mathbf{N}_{u,x} \\ \mathbf{N}_{v,y} \\ \mathbf{N}_{u,x} + \mathbf{N}_{v,y} \end{bmatrix}; \mathbf{B}_2 = \begin{bmatrix} \mathbf{N}_{\varphi x,x} \\ \mathbf{N}_{\varphi y,y} \\ \mathbf{N}_{\varphi x,y} + \mathbf{N}_{\varphi y,x} \end{bmatrix}; \mathbf{B}_3 = \begin{bmatrix} \mathbf{N}_{w,x} + \mathbf{N}_{\varphi x} \\ \mathbf{N}_{w,y} + \mathbf{N}_{\varphi y} \end{bmatrix} \tag{21}$$

The element mass matrix is given by

$$\mathbf{M}_e = \int_{S_e} \mathbf{N}^T \begin{bmatrix} I_1 & 0 & 0 & I_2 & 0 \\ & I_1 & 0 & 0 & I_2 \\ & & I_1 & 0 & 0 \\ & & & I_3 & 0 \\ & & & & I_3 \end{bmatrix} \mathbf{N} dxdy \tag{22}$$

with

$$\mathbf{N} = \left[\mathbf{N}_u^T \quad \mathbf{N}_v^T \quad \mathbf{N}_w^T \quad \mathbf{N}_{\theta x}^T \quad \mathbf{N}_{\theta y}^T \right] \tag{23}$$

$$(I_1, I_2, I_3) = \int_{-h/2}^{h/2} \rho(1, z, z^2) dz \tag{24}$$

Applying Hamilton's principle leads to the motion equation of plates as follows:

$$\mathbf{M}.\ddot{\mathbf{d}} + \mathbf{K}.\mathbf{d} = \mathbf{0} \tag{25}$$

Where $\mathbf{M}, \mathbf{K}, \mathbf{d}$ are the global mass matrix, the global stiffness matrix, the global force vector, and the global displacement vector, respectively.

3. VERIFICATION PROBLEM

Firstly, we consider an SSSS FGP (Case 2) plate with material properties are listed in Table 1. The stiffness factor and non-dimensional frequencies of the plates are introduced by

$$K_1 = \frac{k_1 a^4}{H_b}; K_2 = \frac{k_1 a^2}{H_b}$$

with $H_b = \frac{E_b h^3}{12(1-\upsilon^2)}$ and $\omega^* = \frac{\omega a^2}{h}\sqrt{\frac{\rho_b}{E_b}}$.

The first non-dimensional frequencies of present work in comparsion with [17] where a novel quasi-3D hyperbolic theory is used are shown in Table 2.

Table 1. Material properties of the individual materials

Materials	E (GPa)	υ	ρ (kg/m^3)
Al_2O_3 (ceramic)	380	0.3	3800
Al (metal)	70	0.3	2707

Table 2. The first non-dimensional frequencies of FGP plate

(K_1, K_2)	h/a	ξ = 0			ξ = 0.2		
		Present	[17]	Δ (%)	Present	[17]	Δ (%)
(100, 100)	0.05	15.390	15.439	0.31	16.330	16.320	0.06
	0.10	15.230	15.245	0.09	16.165	16.148	0.11
	0.15	14.968	14.966	0.01	15.919	15.895	0.15
	0.20	14.666	14.640	0.18	15.623	15.595	0.18

Secondly, the plates are partially supported by a Winkler foundation [18] as displayed in Fig. 3. Parameters of the isotropic plate as L_x = 2m, L_y = 1m, h = 0.01m, E = 200GPa, υ = 0.3, and ρ = 7850kg/m^3. The first non-dimensional natural frequencies of the present work compared to those of Motaghian et al. The publication where the analytical solution are listed in Table 3. It can be observed that the numerical results in our work are compared to those of Ref. It can be seen that the erros of the two numerical results are less than 2%. The comparison results given above allow to belive in the accuracy and reliability of the method and calculation programme proposed.

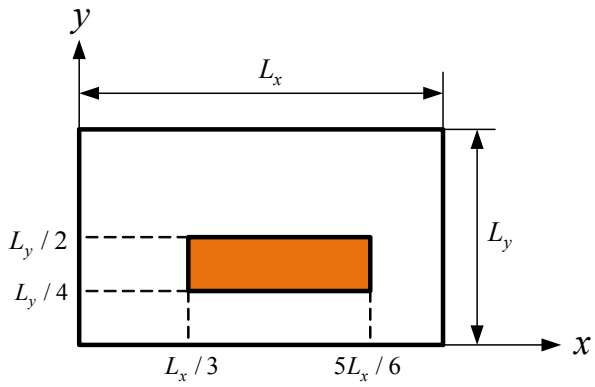

Fig. 3. The plate is partially supported by EF

Table 3. Non-dimensional natural frequencies of plates

Boundary condition		SSSS			CCCC		
K_1	ω_i^*	Present	[18]	Δ (%)	Present	[18]	Δ (%)
10	ω_1^*	5.0256	5.003	0.45	10.2650	10.295	0.29
	ω_2^*	8.0390	8.001	0.47	13.2832	13.348	0.49
	ω_3^*	13.0950	13.00	1.73	18.6812	18.782	0.54
	ω_4^*	17.1712	17.00	1.00	26.0202	26.226	0.78
	ω_5^*	20.327	20.00	1.64	30.1920	29.853	1.14

4. NUMERICAL RESULTS

In this section, the free vibration of FGP plates is considered. The geometry parameters of the FGP plate are b/a = 2 (the value of a is fixed) with material properties as shown in Table 1 and porosity volume fraction ξ = 0.5, volume fraction index k = 1, values of parameters $K_1 = K_2 = 100$. The non-dimensional parameters are taken as in section 3.

Fig. 4 presents the first mode shape of the SSSS FGP plates with the different cases of porosity distribution and types of EF while Fig. 5 shows the first four mode shape of the CCCC FGP (case 1) plates with types 1 of the EF. It can be found that with the same BC and the porosity distribution, the first natural frequency of the FGP plate is placed on the EF type 1 is larger than the first natural frequency of the FGP plate placed on the EF type 2. We can also be concluded that the mode shape of the FGP plate is not symmetric because the stiffness at each position of the plate has different values. The maximum displacement of the mode shapes is traveled to the location of the plate not supported by foundations.

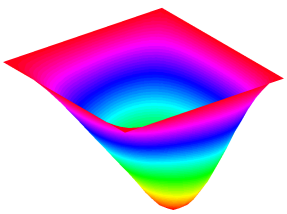

(a) Case 1, Type 1, $\omega_1^* = 9.4610$

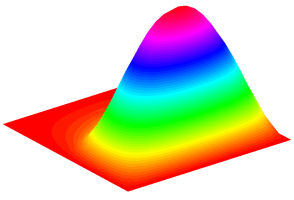

(b) Case 1, Type 2, $\omega_1^* = 6.1065$

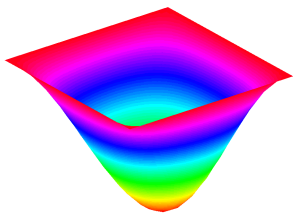

(c) Case 2, Type 1, $\omega_1^* = 9.7116$

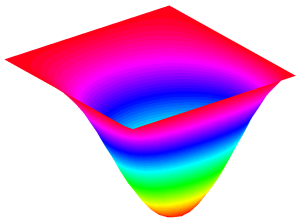

(d) Case 2, Type 2, $\omega_1^* = 8.2783$

Fig. 4. The first mode shapes of SSSS FGP plates with different cases of porosity distribution and types of EFs

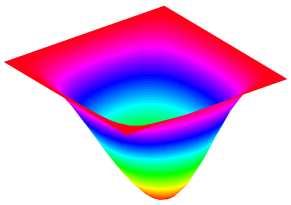

(a) Mode 1, $\omega_1^* = 12.6087$

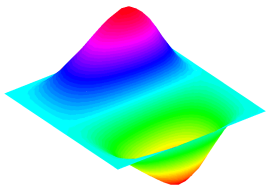

(b) Mode 2, $\omega_2^* = 15.6162$

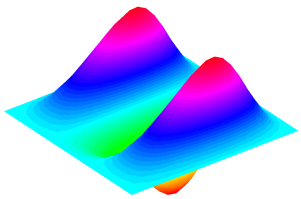

(c) Mode 3, $\omega_3^* = 20.2434$

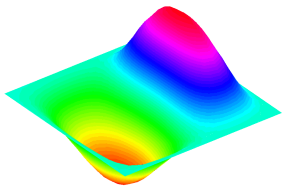

(d) Mode 4, $\omega_4^* = 25.3762$

Fig. 5. The first four mode shapes of the CCCC FGP (Case 1) plate

5. CONCLUSIONS

In this article, the free vibration of the FGP plate partially supported by EF is studied by using the FEM based on Mindlin plate theory. The obtained numerical results of the present approach are compared to other available solutions. From the proposed formulation and the numerical results, we can withdraw some following points:

- The FGP plates resting on different types of EF lead to various natural frequencies. This shows the partially supported foundation significantly affects the free vibration of plates.
- The foundation stiffness parameters and material properties greatly influence the free vibration of the plate. Adjusting these parameters can control the free vibration of FGP plates.
- The present approach can be developed to investigate the free vibration of the FGP plate partially supported by EF with different shapes which not symmetrical as L-shape, Annular-shape, etc.
- Numerical results in the present work are useful for calculation, designing of FGP plate partially supported by EF in engineering and technologies.

REFERENCES

[1]. Q. Li, D. Wu, X. Chen, L. Liu, Y. Yu, W. Gao, 2018. *Nonlinear vibration and dynamic buckling analyses of sandwich functionally graded porous plate with graphene platelet reinforcement resting on Winkler–Pasternak elastic foundation*. International Journal of Mechanical Sciences 148, 596-610.

[2]. A. Zenkour, A. Radwan, 2018. *Free vibration analysis of multilayered composite and soft core sandwich plates resting on Winkler-Pasternak foundations*. Journal of Sandwich Structures & Materials 20(2), 169-190.

[3] N.D. Duc, D.H. Bich, P.H. Cong, 2016. *Nonlinear thermal dynamic response of shear deformable FGM plates on elastic foundations*. Journal of Thermal Stresses 39(3), 278-297.

[4]. N.D. Duc, K. Seung-Eock, P.H. Cong, N.T. Anh, N.D. Khoa, 2017. *Dynamic response and vibration of composite double curved shallow shells with negative Poisson's ratio in auxetic honeycombs core layer on elastic foundations subjected to blast and damping loads*. International Journal of Mechanical Sciences 133, 504-512.

[5]. N. Duc, 2014. *Nonlinear static and dynamic stability of functionally graded plates and shells.* Vietnam: Vietnam Natl Univ Press. Google Scholar.

[6]. A. Mahmoudi, S. Benyoucef, A. Tounsi, A. Benachour, E.A. Adda Bedia, S. Mahmoud, 2019. *A refined quasi-3D shear deformation theory for thermo-mechanical behavior of functionally graded sandwich plates on elastic foundations.* Journal of Sandwich Structures & Materials 21(6), 1906-1929.

[7]. M.H. Omurtag, A. Özütok, A.Y. Aköz, Y. OeZCELİKOeRS, 1997. *Free vibration analysis of Kirchhoff plates resting on elastic foundation by mixed finite element formulation based on Gateaux differential*. International Journal for Numerical Methods in Engineering 40(2), 295-317.

[8]. D. Zhou, Y. Cheung, S. Lo, F. Au, 2004. *Three-dimensional vibration analysis of rectangular thick plates on Pasternak foundation*. International journal for numerical methods in engineering 59(10), 1313-1334.

[9]. A. Ferreira, C. Roque, A. Neves, R. Jorge, C. Soares, 2010. *Analysis of plates on Pasternak foundations by radial basis functions*. Computational Mechanics 46(6), 791-803.

[10]. B. Merazka, A. Bouhadra, A. Menasria, M.M. Selim, A.A. Bousahla, F. Bourada, A. Tounsi, K.H. Benrahou, A. Tounsi, M.M. Al-Zahrani, 2021. *Hygro-thermo-mechanical bending response of FG plates resting on elastic foundations*. Steel and Composite Structures 39(5), 631.

[11]. T.T. Tran, Q.H. Pham, T. Nguyen-Thoi, 2020. *Dynamic Analysis of Functionally Graded Porous Plates Resting on Elastic Foundation Taking into Mass subjected to Moving Loads Using an Edge-Based Smoothed Finite Element Method*. Shock and Vibration 2020.

[12]. T.T. Tran, P.C. Nguyen, Q.H. Pham, 2021. *Vibration analysis of FGM plate in thermal environment resting on elastic foundation using ES-MITC3 element and prediction of ANN*. Case Studies in Thermal Engineering, 100852.

[13]. Seyedemad Motaghian, Massood Mofid, John E. Akin, 2012. *On the free vibration response of rectangular plates, partially supported on elastic foundation.* Applied Mathematical Modelling, 36, 4473–4482.

[14]. D. Shahsavari, M. Shahsavari, L. Li, B. Karami, 2018. *A novel quasi-3D hyperbolic theory for free vibration of FG plates with porosities resting on Winkler/Pasternak/Kerr foundation*. Aerospace Science and Technology 72, 134-149.

[15]. Reddy JN., 2003. *Mechanics of laminated composite plates and shells: theory and analysis*. CRC press.

[16]. T.T. Tran, Q.H. Pham, T. Nguyen-Thoi, 2020. *Dynamic analysis of sandwich auxetic honeycomb plates subjected to moving oscillator load on elastic foundation.* Advances in Materials Science and Engineering 2020.

[17]. Davood Shahsavari, Maryam Shahsavari, Li Li, Behrouz Karami, 2018. *A novel quasi-3D hyperbolic theory for free vibration of FG plates with porosities resting on Winkler/Pasternak/Kerr foundation.* Aerospace Science and Technology, DOI: https://doi.org/10.1016/j.ast.2017.11.004.

[18]. Seyedemad Motaghian, Massood Mofid, John E. Akin, 2012. *On the free vibration response of rectangular plates, partially supported on elastic foundation*. Applied Mathematical Modelling, 36, 4473–4482.

THÔNG TIN TÁC GIẢ

Nguyễn Thị Dung

Khoa Cơ khí, Trường Đại học Kỹ thuật Lê Quý Đôn